

OPEN

Matrix protease production, epithelial-to-mesenchymal transition marker expression and invasion of glioblastoma cells in response to osmotic or hydrostatic pressure

Wenjun Pu¹, Jiawen Qiu¹, Gregory J. Riggins² & Marie-Odile Parat^{1*} 

Both hydrostatic and osmotic pressures are altered in the tumour microenvironment. Glioblastoma (GBM) is a brain tumour with high invasiveness and poor prognosis. We hypothesized that physical and osmotic forces regulate glioblastoma (GBM) invasiveness. The osmotic pressure of GBM cell culture medium was adjusted using sodium chloride or water. Alternatively, cells were subjected to increased hydrostatic force. The proteolytic profile and epithelial–mesenchymal transition (EMT) were investigated using zymography and real-time qPCR. The EMT markers assessed were Snail-1, Snail-2, N-cadherin, Twist and vimentin. Invasion was investigated *in vitro* using extracellular matrix-coated Transwell inserts. In response to osmotic and mechanical pressure, GBM cell lines U87 and U251 and patient-derived neural oncospheres upregulated the expression of urokinase-type plasminogen activator (uPA) and/or matrix metalloproteinases (MMPs) as well as some of the EMT markers tested. The adherent cell lines invaded more when placed in media of increased osmolality. Therefore, GBM respond to osmotic or mechanical pressure by increasing matrix degrading enzyme production, and adopting a phenotype reminiscent of EMT. Better understanding the molecular and cellular mechanisms by which increased pressure promotes GBM invasiveness may help to develop innovative therapeutic approaches.

Physical solid and fluid forces play a key role when solid tumours grow, progress and also respond to therapy¹. Compressive stresses affect cancer cells by promoting invasiveness and metastasis². Tumours are generally hypoperfused, and interstitial fluid pressure is increased compared to normal tissue^{1,3,4} with both increased hydrostatic pressure⁴ and oncotic pressure^{5,6}. Increased interstitial fluid pressure results from abnormal blood and lymphatic vessels, fibrosis and contraction of the matrix by stromal cells⁷. In addition to these stresses common to most solid tumours, brain tumours experience pressure when the tumour grows within a space limited by the skull⁸.

Glioblastoma is the most common primary brain cancer. The average survival time is approximately one year after diagnosis. A major feature of GBM that contributes to its poor prognosis is its high invasiveness. The urokinase-type plasminogen activator (uPA) derives its name from its ability to activate plasminogen into plasmin. While tissue-type plasminogen activator (tPA) plays a role in the fibrinolytic process, uPA is involved in cell migration and tissue remodelling, thereby playing a major role in cancer development and spreading. This role is especially crucial in glioblastoma^{9–11}. Equally important and complementary to the uPA system, MMPs play a key role in the control of the tumour microenvironment and ECM, thereby modulating tumor growth, angiogenesis, invasion and metastasis. Recently reports showed that the MMPs play pivotal roles in the invasiveness of GBM by degrading surrounding tissue, activating signal transduction, releasing ECM-bound growth factors, activating

¹University of Queensland School of Pharmacy, PACE, 20 Cornwall Street, Woolloongabba, QLD, 4102, Australia.

²Department of Neurosurgery, Johns Hopkins University School of Medicine, Baltimore, MD, 21213, USA. *email: m.parat@uq.edu.au

growth factors, increasing tumour cell motility, and promoting angiogenesis^{12–15}. Multiple studies have reported that the expression of higher level of MMPs in brain tumours is associated with increased tumour aggressiveness^{16–18}. Of note, MMP-2 and -9 play a key role in high grade gliomas¹⁹.

There is limited evidence that GBM cells subjected to compressive strain showed increased mRNA expression of both uPA and uPA receptor. We hypothesized that pressure characteristic of the GBM microenvironment, i.e. dysregulated osmotic and mechanical pressure, promote GBM cell invasiveness.

Results

Hyperosmolarity increases GBM matrix protease production. To test the effect of hyper or hypo-osmotic stress on matrix protease production in cell-conditioned medium, cell viability in response to increased (by addition of NaCl) or decreased (by addition of water) osmolality over 6, 12, 24 and 48 h was assessed in preliminary experiments (Supplementary Fig. S1). The osmolalities chosen for further experiments were 285 (control serum-free RPMI), 440, 360 and 260 mOsmol/kg for the U87 and U251 cell lines and 335 (control NeuroCult NS-A Proliferation medium) 415, 375 and 315 mOsmol/kg for the 081024 oncospheres as these did not significantly affect cell viability at 48 h. The urokinase type plasminogen activator (uPA) production was tested using casein plasminogen zymography of the 48 h conditioned medium (Fig. 1a). While hypoosmotic stress had essentially no effect on uPA production, there was an increase in uPA in response to hyperosmolarity which was more dramatic in the conditioned medium of the adherent cell lines compared to that of the oncospheres. Densitometric quantification revealed that uPA was increased 2–3 fold in U87, 3–4 fold in U251, and by ~50% in 081024 cells (Fig. 1b) by the highest hyper-osmolality (440 and 415 mOsmol/kg for adherent and oncosphere cells, respectively). The increased uPA production under hyperosmolar conditions was confirmed using ELISA quantification of uPA in the conditioned medium (Fig. 1c). Furthermore, the expression of uPA mRNA was tested in cells after 48 h exposure to hyper or hypoosmotic stress and confirmed increased expression of uPA in the adherent cells (although statistical significance was reached only with the U251 cells) (Fig. 1d). In contrast, the mRNA expression of uPA receptor was unchanged (data not shown). Increased mRNA expression of uPA in 415 mOsmol/kg medium was confirmed in two additional oncosphere cell lines, JHH136 and 2010.016 A (Supplementary Fig. S2).

We further assessed the production of gelatinases in GBM cells exposed to osmotic stress. At least one gelatinase was increased in the conditioned medium of all cells exposed to hyperosmotic media (Fig. 2a,b and Supplementary Fig. S3a). In addition, hypoosmotic stress increased MMP-2 in U87 cells and MMP-9 in U251 cells. An increased expression of MMP-9 mRNA was seen in adherent cells at 440 mOsmol/kg and in the 081024 oncospheres at 375 and 415 mOsmol/kg (Fig. 2c). Together these results indicate that GBM cells respond to osmotic pressure by an increase in matrix degrading enzyme expression, and the intensity of this response is cell line- and enzyme-specific.

Hyperosmolarity-induced matrix protease production is not a common response of all cancer cells.

We next tested whether non GBM cancer cells similarly responded to increased osmolality by producing more uPA, MMP-2 and MMP-9. We tested the response of the prostate cancer cell line DU145, and breast cancer cell lines MDA-MB-231 and MDA-MB-468 (Supplementary Fig. S4). While DU145 cells grow in RPMI medium and the addition of 1 and 2% V/V 5 M NaCl results in an increase of osmolality from 285 to 360 and 440 mOsmol/kg, respectively, the MDA-MB-231 and -468 cells grow in DMEM and the addition of 1 and 2% V/V 5 M NaCl results in an increase of osmolality from 350 to 430 and 510 mOsmol/kg, respectively. Analysis of the conditioned medium by casein plasminogen zymography (Supplementary Fig. S4a) and gelatin zymography (Fig. S4 b) did not reveal any increase in proteases. On the contrary there decreased uPA was apparent in breast cancer cells MDA-MB-231 and -468 at 510 mOsmol/kg and decreased MMP-2 production in MDA-MB-468 at both 430 and 510 mOsmol/kg. MMP-9 was undetectable in these cell lines. These results indicate that pressure-induced increase in matrix degrading proteases is not a feature of all cancer cell lines.

Hyperosmolarity promotes GBM invasiveness.

To test whether osmotic stress-induced changes in matrix protease production translated into increased invasiveness, we subjected cells to osmotic stress while invading through extracellular matrix protein-coated inserts. Representative images of stained cells on the lower surface of filters and quantification of the number of invaded cells (Fig. 3a) clearly show that hyperosmotic stress promotes invasion of GBM adherent cell lines. Invasiveness is one of the features of the mesenchymal phenotype that is adopted by aggressive tumor cells including gliomas²⁰. We assessed the expression of EMT markers^{20–23} Snail-1, Snail-2 (Slug), Twist, vimentin N-cadherin (CDH2), ZEB1 and ZEB2 in cells exposed to control or hyperosmotic medium for 48 h. The mRNA expression of EMT markers Snail-1, Slug and N-cadherin was increased by exposure of the adherent cell lines to hyperosmolar media (albeit statistical significance was seen for only some of the markers) while ZEB1 and ZEB2 were induced by hyperosmolarity in the 081024 oncospheres (Fig. 3b). Snail-1, Slug and N-cadherin as well as ZEB1 and ZEB2 were increased in the 2010.016 A oncosphere cell line (Supplementary Fig. S2). Therefore our results indicate that GBM cells respond to osmotic pressure by an increase in EMT marker expression, with cell line and marker specificity.

Hydrostatic pressure increases matrix protease production and EMT marker expression by GBM cells.

GBM cells are subjected to increasing interstitial fluid pressure as the tumour grows²⁴. We tested the effect of increased hydrostatic pressure on matrix protease production. Cells exposed to 30 mmHg over 48 h exhibited a slight increase in uPA production in the conditioned medium, which was statistically significant for U87 cells and 081024 oncospheres (Fig. 4a,b). This increase was also seen at the mRNA level in the adherent cell lines (Fig. 4c). Gelatin zymography detected an increased production of MMP-2 and MMP-9 only in the oncospheres (Fig. 5a,b) while increased MMP-2 and MMP-9 mRNA was apparent in U87 cells only (Fig. 5c). The setup employed did not allow us to test the effect of increased hydrostatic pressure on invasion through BME-coated inserts (Transwells), however we quantified the expression of the EMT markers Snail-1, Snail-2 (Slug), Twist,

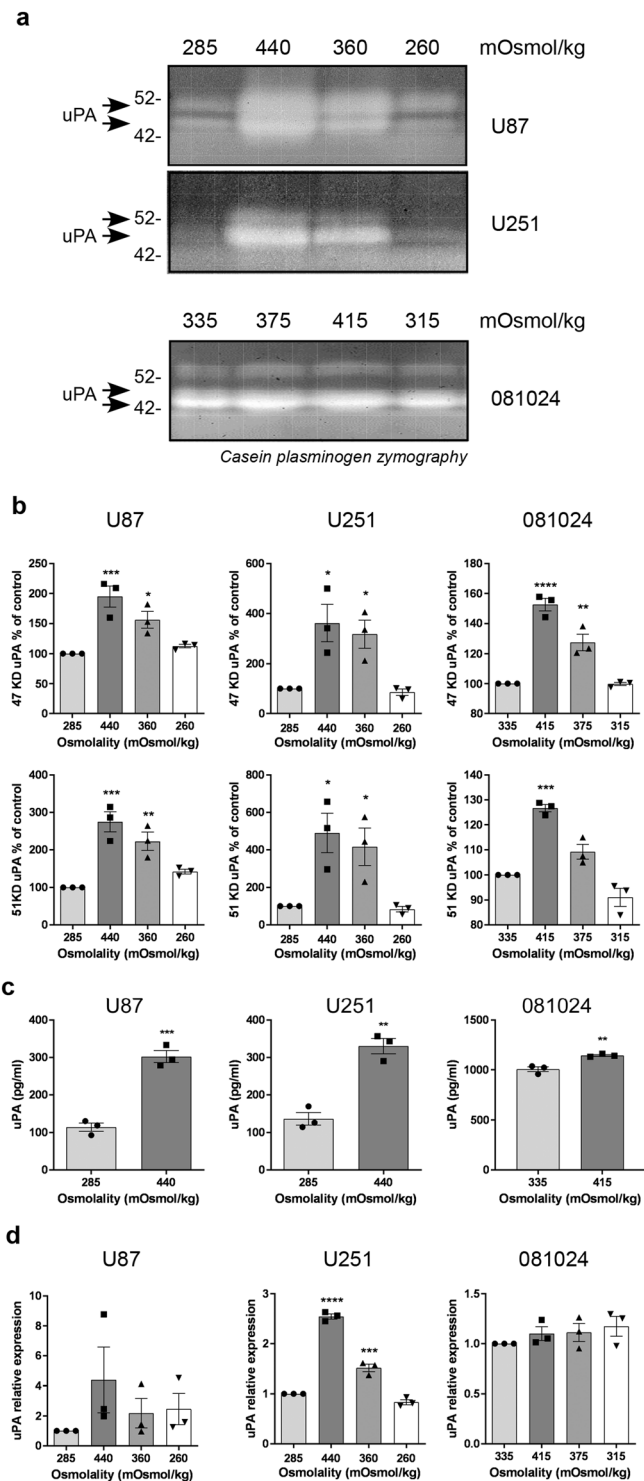


Figure 1. Effect of osmotic pressure on uPA production by GBM adherent and neurosphere cells. **(a)** Conditioned media of cells exposed to control (285 mOsmol/kg) hyper (440 or 360 mOsmol/kg) or hypoosmotic stress (260 mOsmol/kg) were analysed by casein plasminogen zymography. **(b)** Densitometric quantitation of the 47 KD and 51 KD bands corresponding to uPA **(c)** ELISA quantification of uPA in the conditioned medium of GBM cell lines subjected to normo- or hyper-osmolality **(d)** Effect of osmotic pressure on uPA mRNA expression. All results are expressed as mean \pm SEM of $n = 3$ independent experiments, * $p < 0.05$, ** $p < 0.01$, *** $p < 0.001$, **** $p < 0.0001$, one way ANOVA analysis with Dunnett's multiple comparisons test.

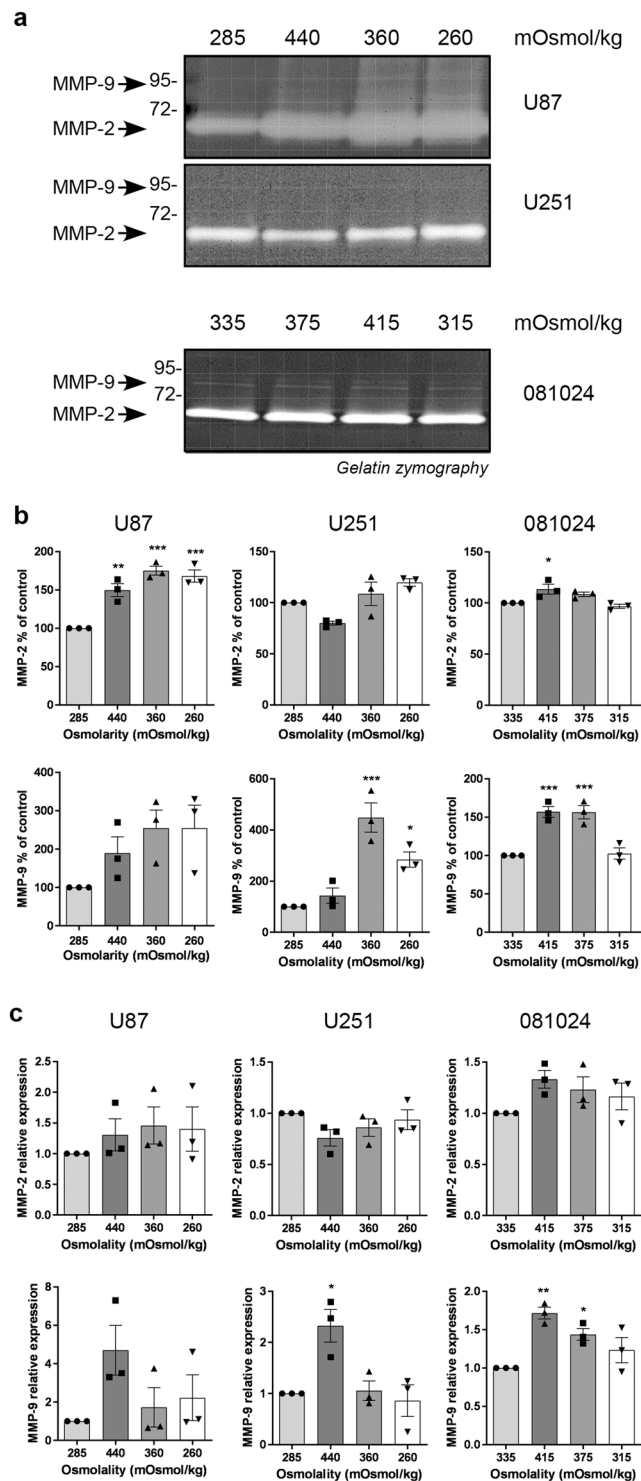


Figure 2. Effect of osmotic pressure on MMP-2 and MMP-9 production by GBM adherent and neurosphere cells. **(a)** Conditioned media of cells exposed to control (285 mOsmol/kg) hyper (440 or 360 mOsmol/kg) or hypoosmotic stress (260 mOsmol/kg) were analysed by gelatin zymography. **(b)** Densitometric quantitation of MMP-2 and MMP-9 produced in the conditioned medium. **(c)** Effect of osmotic pressure on MMP-2 and MMP-9 mRNA expression. All results are expressed as mean \pm SEM of $n = 3$ independent experiments, * $p < 0.05$, ** $p < 0.01$, *** $p < 0.001$, one way ANOVA analysis with Dunnett's multiple comparisons test.

vimentin N-cadherin (CDH-2) ZEB1 and ZEB2 in cells exposed to 30 mmHg compared to control cells (Fig. 6). Expression of these markers was inconsistently increased (although only by $\sim 50\%$) in adherent (Fig. 6a,b) and oncosphere (Fig. 6c) cells. These results show that hydrostatic pressure increased at clinically relevant levels *in vitro* enhances some EMT markers in GBM cells.

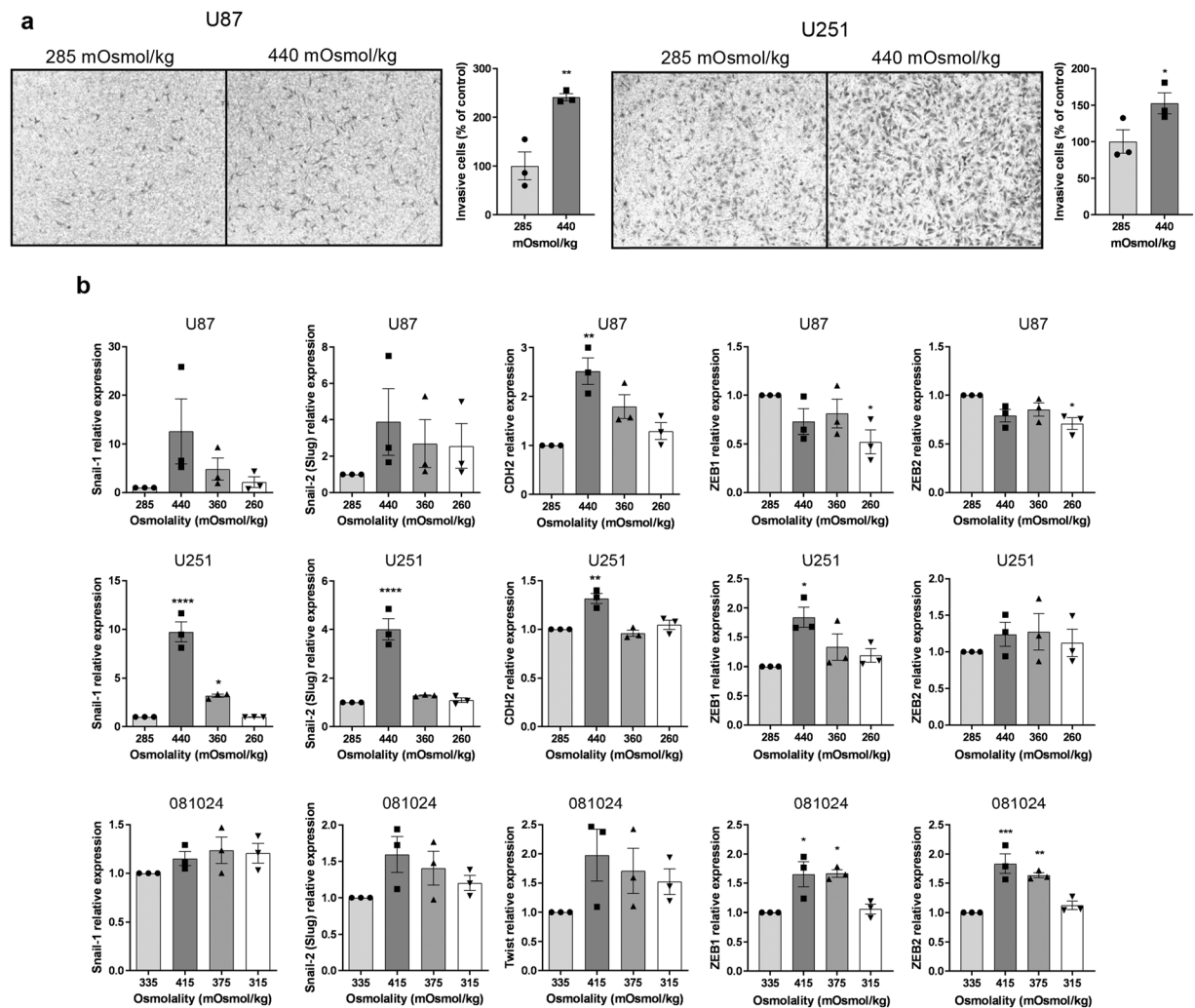


Figure 3. Effect of osmotic pressure on U251 and U87 *in vitro* invasion potential. **(a)** Cell invasion through Matrigel-coated Transwells was determined in control (285 mOsmol/kg) or hyperosmotic (440 mOsmol/kg) media. Representative micrographs with crystal violet-stained cells are shown. Quantitation of invaded cells is shown as percent of normo-osmotic control. Results are expressed as mean \pm SEM of $n = 3$ independent experiments, * $p < 0.05$, ** $p < 0.01$, unpaired Student *t* test. **(b)** mRNA expression of EMT markers in U87 U251 and 081024 cells after 48 h of exposure to control (285 mOsmol/kg for adherent cells, 335 mOsmol/kg for oncospheres) hyper or hypoosmotic stress. All results are expressed relative to cells incubated in normo-osmotic medium as mean \pm SEM of $n = 3$ independent experiments, * $p < 0.05$, ** $p < 0.01$, **** $p < 0.0001$, one way ANOVA analysis with Dunnett's multiple comparisons test.

Discussion

Our experiments show that GBM cells can respond to pressure by increasing their invasive potential. Tumours are exposed to alterations in hydrostatic pressure⁴ and oncotic pressure^{5,6}. In addition, as GBM grows within the confines of the skull, GBM cells are exposed to elevated intracranial pressure compressing the tumour. It has long been known that intracranial pressure is increased in patients with brain tumours as measured *via* cerebrospinal fluid pressure (CSFP). In 18 patients with primary or metastatic brain tumours, mean cerebrospinal fluid pressures of ~ 30 mmHg were recorded, with plateau waves of up to 100 mmHg⁸. In comparison, CSFP at lumbar puncture in patients lying down on their side is considered normal at ~ 10 mmHg²⁵, with normal values proposed to be 4.4 to 18.4 mmHg²⁶. The hydrostatic pressure that cells are exposed to in our study (30 mmHg) is thus clinically relevant. The tumour microenvironment is also characterized by high interstitial colloid osmotic pressure⁷. Using magnetic resonance spectroscopy, the concentration of myoinositol, an organic osmolyte indicative of cell metabolic reaction to osmotic changes into the brain, was shown to be lower in GBM compared to control tissue, to increase after bevacizumab treatment (which normalizes the vasculature and reduces the oedema), and to correlate with better overall survival of the patients²⁷. Interstitial fluid pressure reduction (via strategies such as induction of endogenous antisecretory factor (AF) or administration of exogenous AF peptide) improved the outcome of GBM in patient-derived xenograft mouse experimental models²⁴ and blocked compression-induced proliferation of GBM oncospheres²⁴.

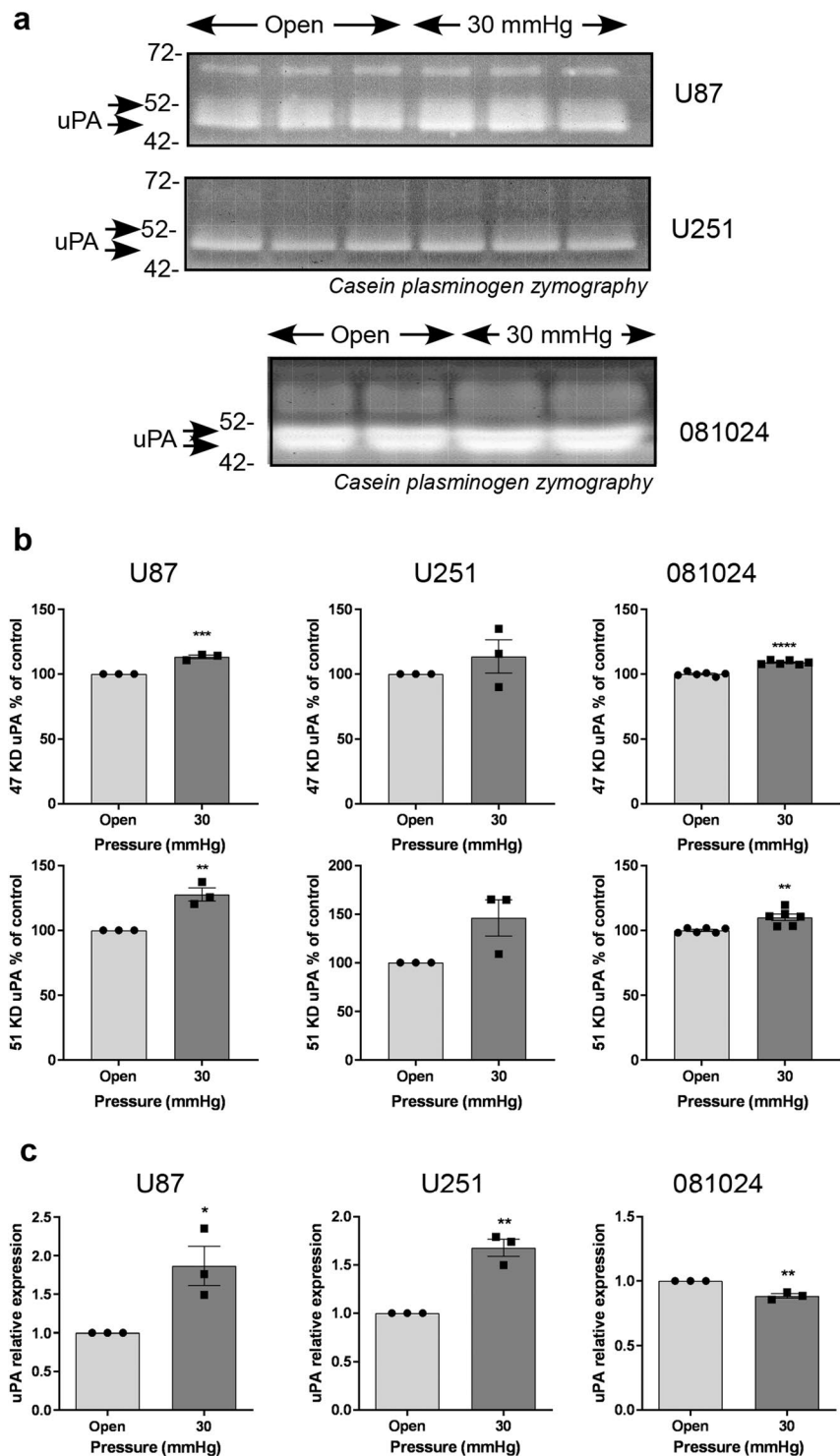


Figure 4. Effect of hydrostatic pressure on uPA production by GBM adherent and neurosphere cells. **(a)** Conditioned media of cells exposed to hydrostatic pressure for 48 h were analysed by casein plasminogen zymography. **(b)** Densitometric quantitation of the 47 KD and 51 KD bands corresponding to uPA. **(c)** Effect of hydrostatic pressure on uPA mRNA expression. All results are expressed as mean \pm SEM of $n = 3$ independent experiments, * $p < 0.05$, ** $p < 0.01$, *** $p < 0.001$, **** $p < 0.0001$, unpaired Student t test.

Hyper and hypo-osmolar stress can affect cell processes including signal transduction, ion homeostasis, volume regulatory processes, cytoskeletal organisation, cell cycle and energy metabolism, with a significant proportion of regulatory processes common to both types of stress²⁸. Changes in volume and shape have been shown to contribute to GBM active migration through brain tissue²⁹. GBM cells benefit from a number of

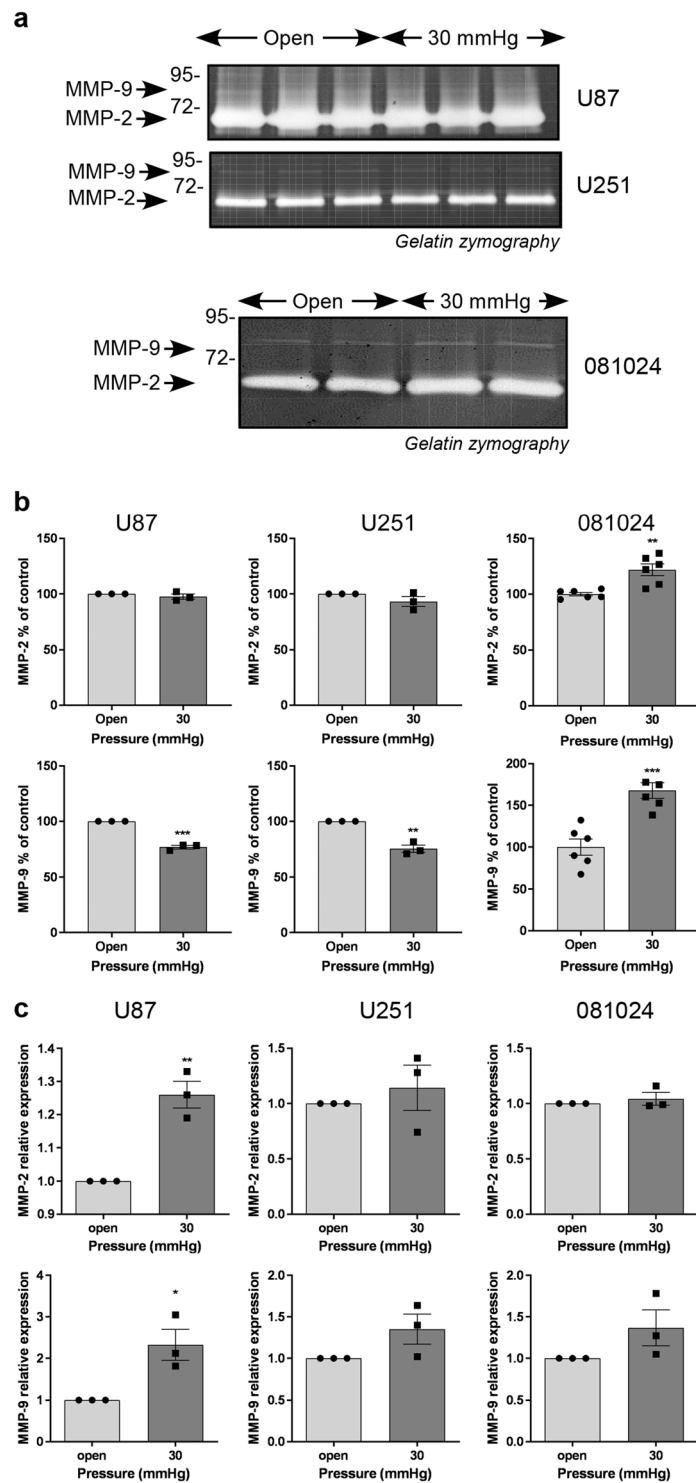


Figure 5. Effect of hydrostatic pressure on matrix metalloproteinase production by GBM adherent and neurosphere cells. **(a)** Conditioned media of cells exposed to hydrostatic pressure for 48 h were analysed by gelatin zymography. **(b)** Densitometric quantitation of MMP-2 and MMP-9 produced in the conditioned medium. **(c)** Effect of hydrostatic pressure on MMP-2 and MMP-9 mRNA expression. All results are expressed as mean \pm SEM of $n = 3$ independent experiments, * $p < 0.05$, ** $p < 0.01$, *** $p < 0.001$, unpaired Student t test.

mechanisms allowing them cells to reduce their volume, including volume activated chloride currents^{30,31}. In *in vitro* experiments, hyperosmotic stress by addition of dextran molecules to the culture medium was shown to trigger morphological transition into an elongated (or lower circularity ratio) shape³². We also tested the effect of hypo-osmotic stress on pro-invasive parameters in light of previous research showing that GBM cells swell in response to hypoxia³³ and that they withstand cell swelling in response to extreme hypoosmotic stress³⁴.

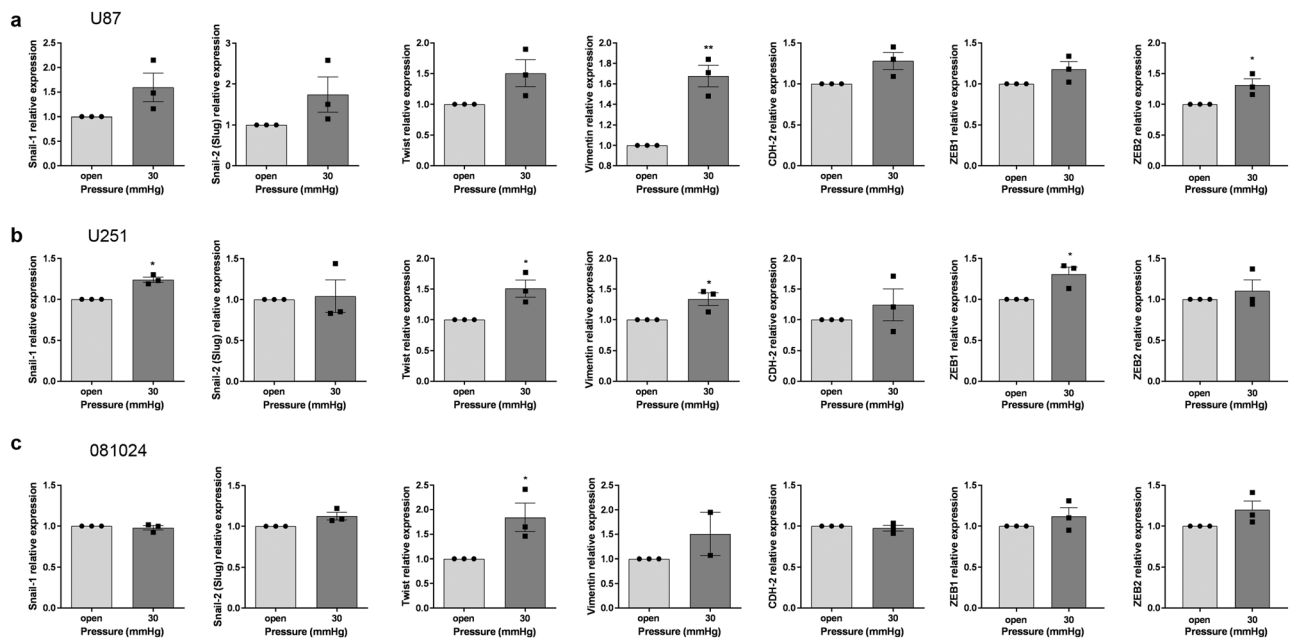


Figure 6. Effect of hydrostatic pressure on EMT marker expression by GBM adherent and neurosphere cells. The mRNA expression of EMT markers was quantified using qRT-PCR in (a) U87 and (b) U251 cells after 48 h of hydrostatic pressure as indicated. (c) The mRNA expression of EMT markers was quantified using qRT-PCR in oncosphere cells after 48 h of hydrostatic pressure as indicated. All results are expressed as mean \pm SEM of $n = 3$ independent experiments, * $p < 0.05$, ** $p < 0.01$, unpaired Student t test.

Our experiments show that hyper- and hypo-osmolarity reduced cell viability at early time points but the cells seemed to recover by the 48 h time point (Supplementary Fig. S1). A biphasic effect of osmotic stress on cell cycle has been studied, albeit at different time points: in hypo-osmotic or hyperosmotic cell culture medium, T98G adherent GBM cells showed an increased fraction of cells in S phase, and a decreased fraction of cells in G1 phase compared to cells grown in isotonic medium at 3 days³². However, this figure was reversed after 6 days³². Our results indicate a minimal impact of hypo-osmolar medium exposure on matrix-degrading enzymes and EMT marker expression (except for an increase in MMP2 in U87, and MMP9 in U251, Fig. 2b). The time course of cell response to swelling may not match the time point at which we analysed the conditioned medium for proteases and the cell lysates for mRNA expression of markers (i.e. 48 h).

Although our results are not uniformly showing an increase of each of the invasive markers tested in all of the cell lines tested, the increase in uPA and/or gelatinase seen in some of the GBM cells exposed to osmotic or hydrostatic pressure is in agreement with previous results showing that GBM cells placed in agarose hydrogels and exposed to 50% compressive strain showed increased mRNA expression of both uPA and uPA receptor by a factor 2–3, as well as cathepsin B and PAI2³⁵. In contrast, transcriptional profiling of patient-derived GBM showed that compression (30%) altered the expression of numerous genes, especially those involved in translational control, stress response and solute transport, however neither uPA nor gelatinases were found to be increased at the mRNA level in that study²⁴. Our work indicates that GBM reacts to pressure by an increased ability to invade. This could be important in the clinic, with alleviating the pressure, or targeting the mechanism(s) by which pressure promotes GBM invasiveness, as approaches to GBM therapy instead of inhibiting the production or activity of key matrix-degrading enzymes³⁶. This is a realistic approach since decreased intracranial pressure can be achieved by antiangiogenic therapies or high dose dexamethasone⁸.

Our experiments show qualitative and quantitative differences in the response to pressure between oncospheres and adherent cell lines. Oncospheres derived directly from primary GBM are known to differ from adherent cell lines and are proposed to better recapitulate the gene expression patterns and *in vivo* biology of human tumours³⁷. Furthermore, their response to pressure may be affected by the fact that they grow as floating clumps. When adherent cell lines are exposed to pressure as a monolayer on a culture dish or flask, it is reasonable to speculate that the entire cell surface would be exposed to the treatment. In contrast, the morphology of cells in neurospheres (i.e. an aggregate or cluster of multiple cells) tends towards large clusters, which may restrict exposure to treatment to cells at the surface of the cluster. Overall, both the adherent cell lines and the oncospheres present disadvantages that limit the extrapolation of our results to *in situ* GBM, but their combined use mitigates these limitations. Future experiments will unveil the mechanism(s) transforming the pressure cues into a signalling program that increases invasiveness. Candidate mechanosensory proteins include integrins, growth factor receptors, stretch activated ion channels³⁸ aquaporins and other solute transport molecules whose expression is dysregulated in GBM³⁹, and caveola-forming proteins^{40,41}.

Methods

Materials. RPMI-1640 medium, Dulbecco's Modified Eagle Medium, trypsin-EDTA, penicillin/streptomycin, Coomassie brilliant blue R-250, Pierce BCA Protein Assay Kit and real-time PCR reagents were purchased from Life Technologies (Melbourne, VIC, Australia). The 40% acrylamide/bis solution was from Bio-Rad (Gladesville, NSW, Australia). CultreCoat 24 well plates with BME-coated inserts and CultreCoat 96 well medium BME cell invasion assay kits were from Bio Scientific Pty. Ltd (Sydney, NSW, Australia). NeuroCult NS-A proliferation kit (human), heparin solution, human recombinant bFGF and human recombinant EGF were purchased from Stemcell Technologies Australia (Tullamarine, VIC, Australia). Other reagents were purchased from Sigma-Aldrich (Castle Hill, NSW, Australia) unless otherwise specified.

Cell culture. Human adherent GBM cell lines U87 and U251 were cultured in RPMI medium supplemented with 5% (v/v) FBS, 100 U/ml penicillin and 100 µg/ml streptomycin. Human prostate cancer DU145 cell line was cultured in RPMI medium with 10% (v/v) FBS, 100 U/ml penicillin and 100 µg/ml streptomycin. Human breast cancer cell lines MDA-MB-231 and MDA-MB-468 were cultured in DMEM medium supplemented with 10% (v/v) FBS, 100 U/ml penicillin and 100 µg/ml streptomycin. Human neurosphere cell lines 081024, JHH136 and 2010.016 A were cultured in NeuroCult NS-A Proliferation medium with 0.2% (v/v) heparin, 20 ng/ml EGF and 10 ng/ml FGF. All cell lines were incubated at 37 °C in a humidified atmosphere with 5% CO₂.

Osmolality measurement. The different osmolality media were prepared by adding different volumes of sterile-filtered 5 mol/L NaCl or sterile water. The osmolality of resulting media was measured using an Osmomat 3000 basic freezing point osmometer (Gally) calibrated using 300 mOsmol/kg and 500 mOsmol/kg standards.

Osmotic stress. 1.0×10^6 cells were seeded in 12 well plates and incubated at 37 °C with 5% CO₂ for 24 hours. After 24 hours, cells were rinsed twice with serum-free medium and 1 ml of serum-free medium of different osmolality was added to each well and incubated for 48 h. The medium was collected and centrifuged at 1,000 × rpm for 5 min, then stored at –80 °C until analysis.

Hydrostatic pressure treatment. 5.0×10^6 cells were seeded in T25 flasks and incubated at 37 °C with 5% CO₂ for 24 hours. Cells were rinsed with serum-free medium twice and incubated in 3 ml of serum-free medium containing 4-(2-hydroxyethyl)-1-piperazineethanesulfonic acid (HEPES) at a final concentration of 25 µM. The flask screwcap was fitted with a three-way stopcock and a sphygmomanometer was used to increase the pressure inside the flask to 30 mmHg. The pressure was verified using the sphygmomanometer at the end of the 48 h incubation. Flasks with a ventilated cap were used as unpressured control. The medium was collected and centrifuged at 1,000 × rpm for 5 min, then stored at –80 °C until analysis.

MTT assay. The cell viability was tested using the 3-[4,5-dimethylthiazole-2-yl]-2,5-diphenyltetrazolium bromide (MTT) assay as previous described⁴². Background absorbance was subtracted and results expressed as the % viability of control cells.

In gel zymography. The production of uPA, MMP-2 and MMP-9 in response to pressure treatment were measured by casein-plasminogen zymography and gelatin zymography as previous described⁴⁰. Equal protein amounts of conditioned media were loaded in each well. The gels were scanned and uPA, MMP-2 and MMP-9 were quantified by densitometry using Image J (v1.48) software.

Quantitative RT-PCR. The mRNA expression of specific genes and epithelial to mesenchymal transition (EMT) markers was measured by real-time reverse transcriptase polymerase chain reaction (real time RT-PCR) as previously described⁴⁰. The primers of target genes were TaqMan gene expression assay for human PLAU (Hs01547054_m1), MMP-2 (Hs01548727_m1), MMP-9 (Hs00957562_m1), Snail-1 (Hs00195591_m1), Snail-2 (Hs00161904_m1), N-cadherin (Hs00983056_m1), Twist (Hs01675818_s1), Vimentin (Hs00185584_m1), ZEB1 (Hs01566408_m1) and ZEB2 (Hs00207691_m1). Relative quantification was done by reference to 18S ribosomal RNA (18S rRNA) and analysed using the comparative critical threshold (Ct) method⁴³.

Cell invasion assay. Cell invasion was determined using CultreCoat 24 well plates with BME-coated Inserts as previously described⁴⁴. The crystal violet-stained cells were imaged using a Leica DFC 295 microscope (10×/0.22) with LAS V4.5 software. The invaded cells were counted by Image J (v1.48) software. Alternatively, cell invasion was determined using CultreCoat 96 well medium BME cell Invasion assay with 2% (V/V) serum in the bottom well as per manufacturer's instructions. The same osmolality was applied in both the upper and lower chambers.

Statistical analysis. Statistical analysis was carried out using GraphPad Prism software (v. 8.01). P-value of <0.05 was considered significant. All the data are shown as mean ± SEM and show either replicates or independent experiments as detailed in the figure legends.

Received: 3 October 2019; Accepted: 27 January 2020;

Published online: 14 February 2020

References

- Jain, R. K., Martin, J. D. & Stylianopoulos, T. The role of mechanical forces in tumor growth and therapy. *Annual review of biomedical engineering* **16**, 321–346 (2014).
- Voutouri, C. & Stylianopoulos, T. Evolution of osmotic pressure in solid tumors. *Journal of biomechanics* **47**, 3441–3447 (2014).
- Koumoutsakos, P., Pivkin, I. & Milde, F. The fluid mechanics of cancer and its therapy. *Annual review of fluid mechanics* **45**, 325–355 (2013).

4. Young, J., Llumsden, C. & Stalker, A. The significance of the “tissue pressure” of normal testicular and of neoplastic (Brown-Pearce carcinoma) tissue in the rabbit. *The Journal of pathology and bacteriology* **62**, 313–333 (1950).
5. Jain, R. K. Transport of molecules across tumor vasculature. *Cancer and Metastasis Reviews* **6**, 559–593 (1987).
6. Jain, R. K. Transport of molecules in the tumor interstitium: a review. *Cancer research* **47**, 3039–3051 (1987).
7. Heldin, C.-H., Rubin, K., Pietras, K. & Östman, A. High interstitial fluid pressure—an obstacle in cancer therapy. *Nature Reviews Cancer* **4**, 806–813 (2004).
8. Alberti, E., Hartmann, A., Schütz, H.-J. & Schreckenberger, F. J. The effect of large doses of dexamethasone on the cerebrospinal fluid pressure in patients with supratentorial tumors. **217**, 173–181, <https://doi.org/10.1007/bf00312958> (1978).
9. Mohanam, S. *et al.* Proteolysis and invasiveness of brain tumors: role of urokinase-type plasminogen activator receptor. *Journal of neuro-oncology* **22**, 153–160 (1994).
10. Rustamzadeh, E., Li, C., Doumbia, S., Hall, W. A. & Valleria, D. A. Targeting the over-expressed urokinase-type plasminogen activator receptor on glioblastoma multiforme. *Journal of neuro-oncology* **65**, 63–75 (2003).
11. Candolfi, M. *et al.* Targeted Toxins for Glioblastoma Multiforme: pre-clinical studies and clinical implementation. *Anti-Cancer Agents in Medicinal Chemistry (Formerly Current Medicinal Chemistry-Anti-Cancer Agents)* **11**, 729–738 (2011).
12. Giannelli, G., Falk-Marzillier, J., Schiraldi, O., Stetler-Stevenson, W. G. & Quaranta, V. Induction of cell migration by matrix metalloproteinase-2 cleavage of laminin-5. *Science* **277**, 225–228 (1997).
13. McCawley, L. J. & Matrisian, L. M. Matrix metalloproteinases: they’re not just for matrix anymore! *Current opinion in cell biology* **13**, 534–540 (2001).
14. Dong, J. *et al.* Metalloproteinase-mediated ligand release regulates autocrine signaling through the epidermal growth factor receptor. *Proceedings of the National Academy of Sciences* **96**, 6235–6240 (1999).
15. Platten, M., Wick, W. & Weller, M. Malignant glioma biology: Role for TGF- β in growth, motility, angiogenesis, and immune escape. *Microscopy research and technique* **52**, 401–410 (2001).
16. Forsyth, P. *et al.* Gelatinase-A (MMP-2), gelatinase-B (MMP-9) and membrane type matrix metalloproteinase-1 (MT1-MMP) are involved in different aspects of the pathophysiology of malignant gliomas. *British journal of cancer* **79**, 1828 (1999).
17. Nakagawa, T., Kubota, T., Kabuto, M., Fujimoto, N. & Okada, Y. Secretion of matrix metalloproteinase-2 (72 kD gelatinase/type IV collagenase= gelatinase A) by malignant human glioma cell lines: implications for the growth and cellular invasion of the extracellular matrix. *Journal of neuro-oncology* **28**, 13–24 (1996).
18. Nakano, A., Tani, E., Miyazaki, K., Yamamoto, Y. & Furuyama, J.-I. Matrix metalloproteinases and tissue inhibitors of metalloproteinases in human gliomas. *Journal of neurosurgery* **83**, 298–307 (1995).
19. Levičar, N., Nutall, R. & Lah, T. Proteases in brain tumour progression. *Acta neurochirurgica* **145**, 825–838 (2003).
20. Iwade, Y. Epithelial-mesenchymal transition in glioblastoma progression. *Oncology letters* **11**, 1615–1620, <https://doi.org/10.3892/ol.2016.4113> (2016).
21. Mikheeva, S. A. *et al.* TWIST1 promotes invasion through mesenchymal change in human glioblastoma. *Molecular Cancer* **9**, 194, <https://doi.org/10.1186/1476-4598-9-194> (2010).
22. Mahabir, R. *et al.* Sustained elevation of Snail promotes glial-mesenchymal transition after irradiation in malignant glioma. *Neuro-Oncology* **16**, 671–685, <https://doi.org/10.1093/neuonc/not239> *J Neuro-Oncology* (2013).
23. Xie, Y.-k. *et al.* CDA-2 induces cell differentiation through suppressing Twist/SLUG signaling via miR-124 in glioma. **110**, 179–186, <https://doi.org/10.1007/s11060-012-0961-x> (2012).
24. Ilkhanizadeh, S. *et al.* Antisecretory Factor-Mediated Inhibition of Cell Volume Dynamics Produces Antitumor Activity in Glioblastoma. *J Molecular Cancer Research* **16**, 777–790, <https://doi.org/10.1158/1541-7786.MCR-17-0413> (2018).
25. Ravussin, P. *et al.* Changes in CSF pressure after mannitol in patients with and without elevated CSF pressure. **69**, 869, <https://doi.org/10.3171/jns.1988.69.6.0869> (1988).
26. Lee, S. C. M. & Lueck, C. J. Cerebrospinal Fluid Pressure in Adults. **34**, 278–283, <https://doi.org/10.1097/wno.000000000000155> (2014).
27. Steidl, E. *et al.* Myoinositol as a Biomarker in Recurrent Glioblastoma Treated with Bevacizumab: A 1H-Magnetic Resonance Spectroscopy Study. *PLOS ONE* **11**, e0168113, <https://doi.org/10.1371/journal.pone.0168113> (2016).
28. Evans, T. G. & Somero, G. N. A microarray-based transcriptomic time-course of hyper- and hypo-osmotic stress signaling events in the euryhaline fish *Gillichthys mirabilis*: osmosensors to effectors. **211**, 3636–3649, <https://doi.org/10.1242/jeb.022160> *J Journal of Experimental Biology* (2008).
29. Watkins, S. & Sontheimer, H. Hydrodynamic Cellular Volume Changes Enable Glioma Cell Invasion. **31**, 17250–17259. *The Journal of Neuroscience*. <https://doi.org/10.1523/JNEUROSCI.3938-11.2011> (2011).
30. Ransom, C. B., O’Neal, J. T. & Sontheimer, H. Volume-Activated Chloride Currents Contribute to the Resting Conductance and Invasive Migration of Human Glioma Cells. *The Journal of Neuroscience* **21**, 7674–7683, <https://doi.org/10.1523/JNEUROSCI.21-19-07674.2001> (2001).
31. Catacuzzeno, L. *et al.* Identification of Key Signaling Molecules Involved in the Activation of the Swelling-Activated Chloride Current in Human Glioblastoma Cells. **247**, 45–55, <https://doi.org/10.1007/s00232-013-9609-9> (2014).
32. Pozzi, G., Marchesi, S., Scita, G., Ambrosi, D. & Ciarletta, P. Mechano-biological model of glioblastoma cells in response to osmotic stress. *Math Biosci Eng* **16**, 2795–2810, <https://doi.org/10.3934/mbe.2019139> (2019).
33. Sforza, L. *et al.* Hypoxia Modulates the Swelling-Activated Cl Current in Human Glioblastoma Cells: Role in Volume Regulation and Cell Survival. **232**, 91–100, <https://doi.org/10.1002/jcp.25393> (2017).
34. Memmel, S. *et al.* Cell Surface Area and Membrane Folding in Glioblastoma Cell Lines Differing in PTEN and p53 Status. *PLOS ONE* **9**, e87052, <https://doi.org/10.1371/journal.pone.0087052> (2014).
35. Demou, Z. Gene Expression Profiles in 3D Tumor Analogs Indicate Compressive Strain Differentially Enhances Metastatic Potential. *Annals of Biomedical Engineering* **38**, 3509–3520 (2010).
36. Hatoum, A., Mohammed, R. & Zakieh, O. The unique invasiveness of glioblastoma and possible drug targets on extracellular matrix. *Cancer Manag Res* **11**, 1843–1855, <https://doi.org/10.2147/CMAR.S186142> (2019).
37. Lee, J. *et al.* Tumor stem cells derived from glioblastomas cultured in bFGF and EGF more closely mirror the phenotype and genotype of primary tumors than do serum-cultured cell lines. *Cancer Cell* **9**, 391–403 (2006).
38. Northey, J. J., Przybyla, L. & Weaver, V. M. Tissue Force Programs Cell Fate and Tumor Aggression. *Cancer Discovery* **7**, 1224–1237, <https://doi.org/10.1158/2159-8290.CD-16-0733> (2017).
39. MARKERT, J. M. *et al.* Differential gene expression profiling in human brain tumors. **5**, 21–33, <https://doi.org/10.1152/physiolgenomics.2001.5.1.21> (2001).
40. Pu, W. *et al.* Correlation of the invasive potential of glioblastoma and expression of caveola-forming proteins caveolin-1 and CAVIN1. **143**, 207–220, <https://doi.org/10.1007/s11060-019-03161-8> (2019).
41. Parat, M. O. & Riggins, G. J. Caveolin-1, caveolae, and glioblastoma. *Neuro Oncol* (2012).
42. Khabbazi, S., Nassar, Z. D., Goumon, Y. & Parat, M.-O. Morphine decreases the pro-angiogenic interaction between breast cancer cells and macrophages *in vitro*. *Scientific Reports* **6**, 31572, <https://doi.org/10.1038/srep31572> (2016).
43. Schmittgen, T. D. & Livak, K. J. Analyzing real-time PCR data by the comparative CT method. *Nat. Protocols* **3**, 1101–1108 (2008).
44. Khabbazi, S., Goumon, Y. & Parat, M. O. Morphine Modulates Interleukin-4- or Breast Cancer Cell-induced Pro-metastatic Activation of Macrophages. *Scientific Reports* **5**, 11389 (2015).

Acknowledgements

We thank Robert G. Parton for insightful discussions and for editing the manuscript, and Jonathan M. Harris for providing his expertise in the field of matrix proteases. This study was supported by funds from the University of Queensland School of Pharmacy.

Author contributions

Study conception and design W.P. and M.O.P. - Experimental work W.P. and J.Q. - Analysis and interpretation of the data W.P. and M.O.P. - Article writing or critical revision W.P., G.J.R. and M.O.P.

Competing interests

The authors declare no competing interests.

Additional information

Supplementary information is available for this paper at <https://doi.org/10.1038/s41598-020-59462-w>.

Correspondence and requests for materials should be addressed to M.-O.P.

Reprints and permissions information is available at www.nature.com/reprints.

Publisher's note Springer Nature remains neutral with regard to jurisdictional claims in published maps and institutional affiliations.



Open Access This article is licensed under a Creative Commons Attribution 4.0 International License, which permits use, sharing, adaptation, distribution and reproduction in any medium or format, as long as you give appropriate credit to the original author(s) and the source, provide a link to the Creative Commons license, and indicate if changes were made. The images or other third party material in this article are included in the article's Creative Commons license, unless indicated otherwise in a credit line to the material. If material is not included in the article's Creative Commons license and your intended use is not permitted by statutory regulation or exceeds the permitted use, you will need to obtain permission directly from the copyright holder. To view a copy of this license, visit <http://creativecommons.org/licenses/by/4.0/>.

© The Author(s) 2020